ROMANIAN JOURNAL OF INFORMATION SCIENCE AND TECHNOLOGY
Volume **14**, Number 4, 2011, 309–323

A Thermal Study on Joule-Heating Induced Effects in Dielectrophoretic Microfilters

Oana Tatiana NEDELCU

National Institute for Research and Development in Microtechnologies (IMT-Bucharest), Romania

E-mail: oana.nedelcu@imt.ro

Abstract. Dielectrophoretic filters are used for separation and detection of cells or microorganisms suspended in liquid media and are based on particles migration in non-uniform electric field provided by microfabricated electrodes. In this paper, thermal effects induced by Joule heating on flow profile and particles distribution by mean of parameter variation with temperature are investigated. The equation system with boundary condition for solving physical quantities such as electric field is described by taking into account the temperature gradient. The models are applied to a microfilter with planar castellated electrodes placed on a channel separation, and numerically solved with simulation software packages. The analyses were made for various set of parameters (as applied voltage and particles size). The results are discussed and compared in terms of temperature influence on electric field, dielectroforetic force, flow profile and spatial concentration distribution of particles inside the separation microchannel.

Keywords: microfilters, dielectrophoresis, thermal effects.

1. Introduction

Dielectrophoresis (DEP) represents the movement of polarisable particles in non-uniform fields and is efficient tools for non-invasive separation and detection of biological cells, macromolecules or viruses [1–5]. The latest development of microfabrication techniques are used to obtain electrodes structures that improve the separation efficiency. Usually, the electrodes are placed on a separation channel surface,

in contact with fluid media, while in the presence of insulator layer the separation dielectrophoretic force can be up to 80 % lower as function of layer thickness. The geometric configurations can be interdigitated, castellated or polynomial configurations of [6–8]. The length has few millimetres, the electrode gap varies between 1–500 μm, and the applied voltage is in the range of 1–40 V at frequencies between 10^2–10^8 Hz. These kinds of microelectrodes have been used to separate, sort, positioning, concentrate, biomolecules as bacteria, virus, DNA and proteins. The particle size varies between 0.01–15 μm and the suspension media can be deionized water having low conductivity or aqueous saline solution with higher conductivity. The suspending media can be deionized water having low conductivity or aqueous saline solution with higher conductivity, and the particle size varies between 0.01–15 μm. This separation method has been further used for bioparticles detection in applications as diagnosis (medical, biological) or drug delivery [9]. Most of reported results on separation effect are obtained from experimental work. The theoretical results (analytical or numerical) in physical quantities distribution (as electric field, flow velocity or particles concentration) are based on several assumption that simplify the mathematical approach. The equation for electric field is usually based on uniform and constant permittivity of medium, while the possible variations with temperature, or influence given by presence of particles are not considered. Also, the equations used for solution flow are incompressible Navier-Stokes and continuity equation applied to carrier fluid properties; the influence of temperature and particles in terms of density, viscosity or drag forces are not taken into account. In this paper we present an analysis of thermal induces effects on dielectrophoretic parameters, flow characteristics and particles diffusion, by mean of variations in permittivity, conductivity, density, viscosity and diffusion coefficient. The models that characterize the thermal variations arising from Joule heating are introduced in equations systems for these phenomena. This approach is numerically solved by complex simulation tools as Comsol Multiphysics that allow extending conventional models by introducing supplementary effects or models variation, and solving coupled physics phenomena. Such models refinements applied to dielectrophoretic microfilters contribute to an improved level of predictions on particles distribution and separation, to understand some effects experimentally observed in the pattern of fluid flow and movement of particles, and also to understand how various forces influence the behavior of fluid and particles and how these can be used to improve the separation efficiency.

2. Theory and models

2.1. Dielectrophoresis

The dielectrophoretic force that act on a particle can be written [10]:

$$\vec{F}_{DEP} = \mathrm{Re}\left[(\vec{p}\cdot\nabla)\,\vec{E}\right], \tag{1}$$

where $\vec{p}$ is induced dipole moment, $\vec{E}$ is the electric field, and Re refers to real part of expression. For spherical particles, the time averaged DEP force is:

$$\vec{F}_{DEP} = \frac{1}{2} V_p \mathrm{Re}(\alpha^*) \nabla \left| \vec{E}_{RMS} \right|^2, \tag{2}$$

where V_p is the volume of one particle, $\vec{E}_{RMS}$ is the root mean square of electric field and and α^* is the particle polarisability, which depends on complex permittivity of medium (ε_m^*) and particles (ε_p^*), and angular frequency of electric field ω:

$$\alpha^* = 3\varepsilon_m \left(\frac{\varepsilon_p^* - \varepsilon_m^*}{\varepsilon_p^* + 2\varepsilon_m^*} \right) = 3\varepsilon_m K, \tag{3}$$

where K is Clausius–Mossotti factor. The complex permittivity for each material is:

$$\varepsilon^* = \varepsilon + \frac{\sigma}{i\omega} = \varepsilon - \frac{i\sigma}{\omega}, \tag{4}$$

where ε is real permittivity σ is the conductivity and i is the imaginary unit.

The dielectrophoretic velocity of spherical particles induced by electric field and φ can be written:

$$\vec{v}_{DEP} = \mu_{DEP} \nabla \left| \vec{E} \right|^2, \tag{5}$$

where $\mu_{DEP} = V_p \alpha / 4\varphi$ is the dielectrophoretic mobility, $\varphi = 6\pi\eta R$ is the Stokes factor, η is the fluid viscosity and R is particle radius. DEP mobility depends on applied frequency by mean of polarisability. Positive mobility leads to particles separation in regions with high electric field, while particles having negative mobility are repelled from these regions. A typical variation of DEP mobility is depicted in figure 1 for polystyrene particles having 1 μm in diameter (conductivity 2×10^{-4} S/m, relative permittivity 2.5 at 20°C) suspended in DI water (relative permittivity 80, conductivity 6.6×10^{-5} S/m at 20°C), for frequencies between 10 Hz–100 MHz.

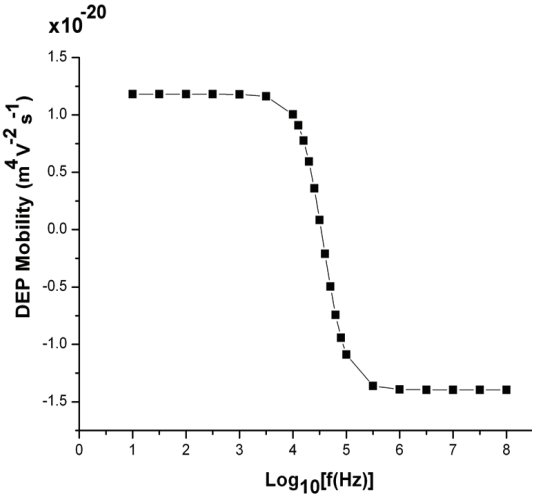

Fig. 1. Variation with frequency of DEP mobility of 1 μm diameter polystyrene particles in DI water.

At frequencies below 1 kHz, the DEP mobility of these particles is near constant around $1.18\times10^{-20}\mathrm{m}^4\mathrm{V}^{-2}\mathrm{s}^{-1}$, it decrease to negative values, for frequencies between 1–100 kHz, and reach its minimum of $-1.39\times10^{-20}\mathrm{m}^4\mathrm{V}^{-2}\mathrm{s}^{-1}$ for higher frequencies. For particles characterized by different parameters (diameter, permittivity or conductivity), the variation of DEP mobility with frequency has similar aspect, although it can be either increasing or decreasing from minimal to maximal frequency, while the extreme mobility values are different. For example, in Figures 2 and 3, DEP mobility variation is depicted for other two cases.

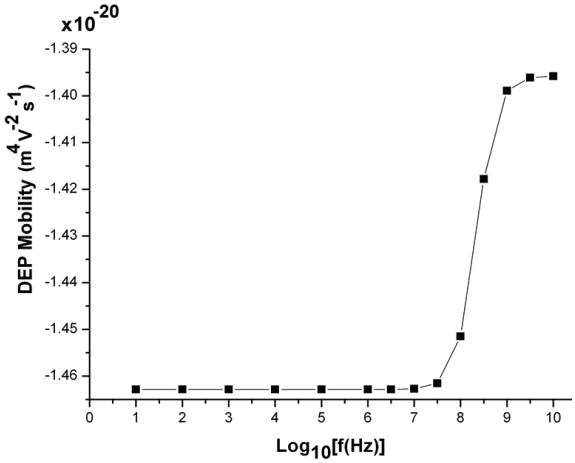

Fig. 2. Variation with frequency of DEP mobility of 1 μm diameter polystyrene particles in saline water (conductivity 1 S/m).

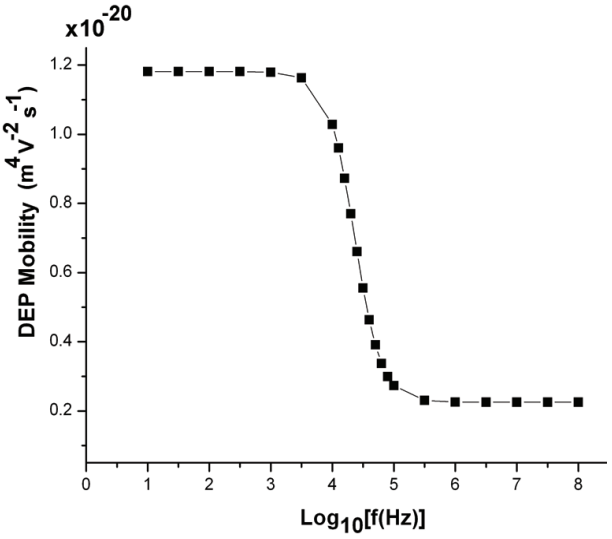

Fig. 3. Variation with frequency of DEP mobility of 1 μm diameter particles with high relative permittivity ($\varepsilon_r = 100$) in DI water.

In Figure 2, DEP mobility of the same polystyrene particles in saline water (conductivity of 1 S/m) increases with frequency, but the values are always negative. In Figure 3, DEP mobility of particles with higher relative permittivity ($\varepsilon_r = 100$) in DI water decreases with frequency, and the values are always positive.

For most types of particles, the positive or negative DEP can be obtained by switching frequency of electric field. Also, different kind of particles can be separated in the same process by choosing the appropriate frequency that induces positive DEP for first kind of particles and negative DEP for the second kind of particles.

2.2. Model for fluid-particle interaction

In theoretical evaluation of flow in DEP microfilters, the presence of particle is not taken into account. To evaluate the influence of particles on fluid flow, we consider $\vec{F}_{DEP}(\vec{x})$ the force acting on one particle in position, given by (2) and an infinitesimal volume V corresponding to point $\vec{x}$, as well as for each particle in V, the DEP force is $\vec{F}_{DEP}(\vec{x})$. The particles in V move trough fluid under a total force given by:

$$\vec{F}_{DEP\_Total} = N \cdot \vec{F}_{DEP}, \tag{6}$$

where N is the number of particles in volume V. By dividing the total DEP force to volume V, we obtain body force that acts on particles in volume V, expressed by force density:

$$\vec{f}_{DEP}(\vec{x}) = c(\vec{x}) N_A \vec{F}_{DEP}. \tag{7}$$

When particles given by $c(\vec{x})$ move in fluid under body force $\vec{f}_{DEP}(\vec{x})$, the reaction force that act on surrounding fluid in volume V is equal to DEP body force, and it has opposite sense:

$$\vec{f}_R(\vec{x}) = -\vec{f}_{DEP}(\vec{x}). \tag{8}$$

The reaction force on fluid media influences flow of fluid in control volume V and in vicinity of V. Consequently, the velocity profile will be modified by comparison to case in that no reaction force is considered [11–12].

2.3. Thermal effects

The electric fields used in particles separation induces changes in temperature by Joule heating. The material parameters that vary with temperature are permittivity, conductivity, density and viscosity of the suspending medium, and also diffusion coefficient of particles. Permittivity has its primary contribution to electric field distribution given by Maxwell equations. Also, permittivity and conductivity contribute to intensity of DEP force by mean of particle polarisability given by (3), and consequently, to intensity of reaction force given by (8). Density and viscosity of medium contribute to flow profile that is modified by temperature changes. In summary, temperature variation induces changes in particles distribution by permittivity and

conductivity via electric field and DEP force, by medium density and viscosity via flow velocity and directly by diffusion coefficient.

The parameters variation can be written as function of a coefficient k:

$$f(T) = f(T_0)\left(1 + \tilde{k} \cdot (T - T_0)\right) \text{ or } \left(\frac{1}{f}\right)\left(\frac{\partial f}{\partial T}\right) = \tilde{k}\left[\mathrm{K}^{-1}\right] \tag{9}$$

For water, permittivity coefficient is $\tilde{k} = 0.004$ and conductivity coefficient is 0.02. Density and viscosity cannot be evaluated with relation (9) since the coefficient is not constant; however, these are known in material properties databases for temperature range 0–100°C, and can be polynomial interpolated when need analytical expressions. The variation of these parameters is illustrated in Figure 4 where the values are related to properties at 20°C. High decrease of viscosity and low decreasing of density with temperature lead to higher values for convective velocity. The decrease in permittivity is connected to higher electric field, while high increase of conductivity influences the dielectrophoretic mobility, force and velocity.

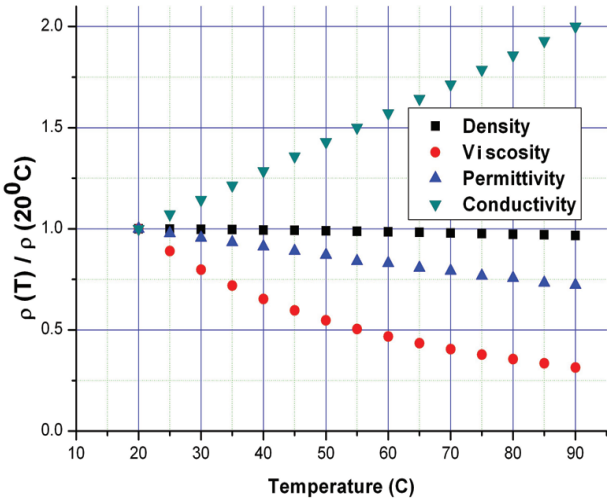

Fig. 4. Thermal variation of water properties.

The influence of temperature on DEP mobility of particles by mean of fluid permittivity and conductivity variation is illustrated in Figure 5 for 1 μm diameter polystyrene particles in DI water. The mobility increase from 1.18119×10^{-20} $\mathrm{m^4V^{-2}s^{-1}}$ at 293 K ($\varepsilon_r = 80$, $\sigma = 6.6 \times 10^{-5}$ S/m) to 2.27536×10^{-20} $\mathrm{m^4V^{-2}s^{-1}}$ at 343 K ($\varepsilon_r = 96$ and $\sigma = 13.2 \times 10^{-5}$ S/m).

Diffusion coefficient of suspending particles in fluid media is [13]:

$$D = \frac{kT}{6\pi\eta\,(T)\,R}, \tag{10}$$

where T is temperature, k – Boltzmann constant, η – fluid viscosity and R the particle radius. The temperature contribute to diffusion coefficient directly and also by mean

of viscosity. A comparison between variation of diffusion coefficient with temperature with and without considering influence of viscosity variation is shown in Figure 6 for particles having 0.1 μm in diameter. Circle dots represents the real variation when decreasing viscosity with temperature is taken into account, and the diffusion coefficient is higher than in case of considering only direct temperature influence, represented by squared dots.

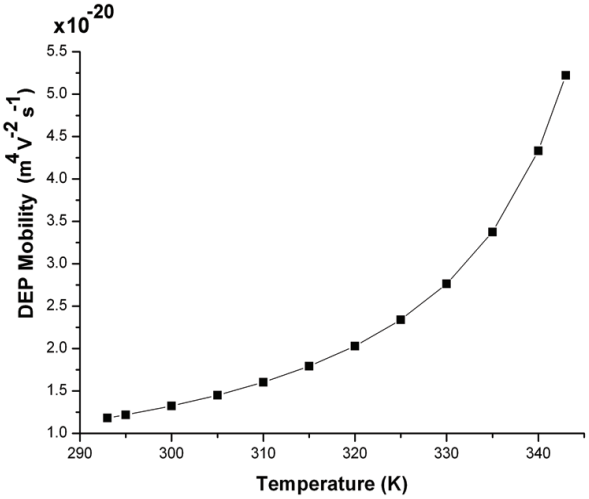

Fig. 5. Temperature variation of DEP mobility of 1 μm diameter polystyrene particles in DI water.

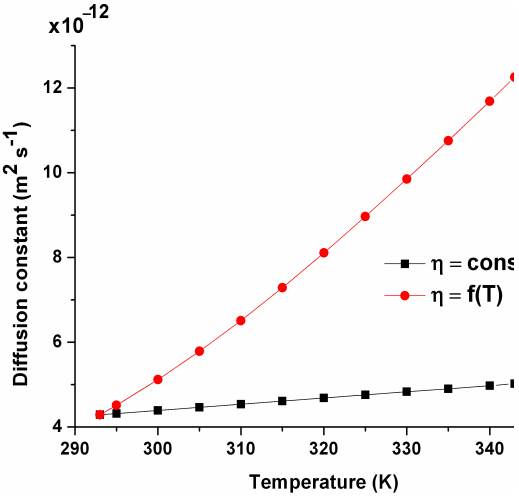

Fig. 6. Thermal variation of diffusion coefficient with and without considering viscosity thermal effect (particles diameter: 0.1 μm).

In this way, temperature effect can be used to separate similar dielectric particles with different diameters by increasing difference between their diffusion coefficients

that will influence the spatial distribution in the channel. This is illustrated in Figure 7, where variation of diffusion coefficient is depicted for particles of 0.1, 0.2 and 1 micrometers in diameter.

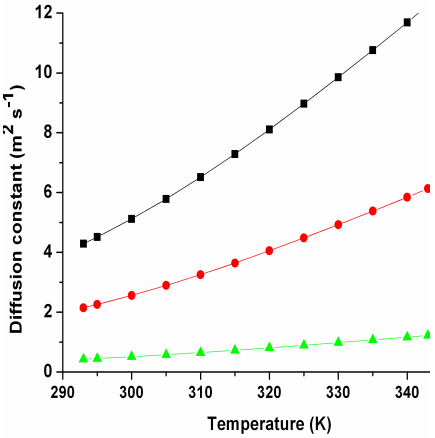

Fig. 7. Temperature variation of diffusion coefficient for particles of 0.1, 0.2 and 1 micrometers in diameter.

3. Results and discussions

Numerical studies were performed using Comsol Multiphysics to obtain solutions based on the proposed models. A 3D channel was considered (100 μm×50 μm×20 μm). Fluid suspending media is deionized water (relative permittivity 80, conductivity 6.6×10^{-5} S/m at 20°C). The particles are polystyrene microspheres (conductivity 2×10^{-4} S/m, relative permittivity 2.5 at 20°C). The electrodes are castellated having 5 μm wide and 5 μm gap and are placed on the top surface (Figure 8).

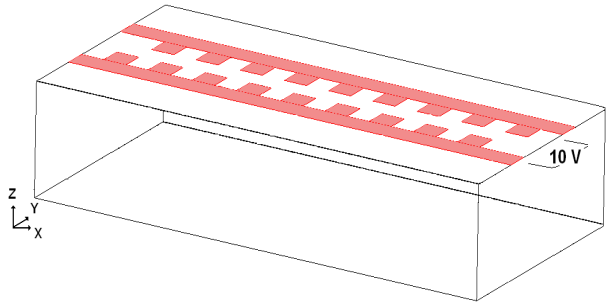

Fig. 8. Separation microchannel and castellated electrodes configuration.

The analyses are based on the following equations [14, 15]:

i) Maxwell equation for electrostatics with electric potential applied between electrodes and insulation on the walls as boundary condition;

ii) Equations for Joule heating given by conservation of electrical charge equation and balance of thermal energy equation;

iii) Navier-Stokes equations for mixture model, considering density and viscosity of the mixture as function of fluid and particles concentration in terms of volume fraction, where fluid density and viscosity are function of temperature. The reaction force on fluid as response to particles dielectrophoretic migration given by relation (8) was introduced as body force. The boundary conditions are given in pressure drop between inlet and outlet and no slip on the channel walls;

iv) Convection-diffusion equation for particles migration in fluid media, where diffusion coefficient is function of temperature and convection velocity is given by flow velocity and DEP velocity. As boundary condition, fixed concentration was set at inlet, insulation on the channel walls and convective flux at outlet.

Electrostatic simulation was performed for 10–50 V applied between electrodes at 100 Hz angular frequency, value that induces positive dielectrophoresis. In Figure 9 the variation of maximum electric field as function of applied voltage is depicted. The values vary from 2.1×10^6 V/m for 10 V to 10.4×10^6 V/m for 50 V.

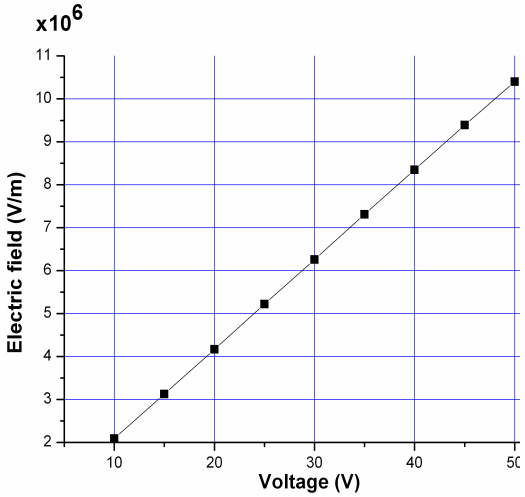

Fig. 9. Maximum electric field variation as function of applied voltage.

The electric field distribution obtained for 20 V is illustrated in Figure 10, in channel volume (a) and in vertical longitudinal section at one electrode edge (b). The values reach 4.17×10^6 V/m at the electrodes edges, and 0.0039×10^6 V/m on the channel bottom.

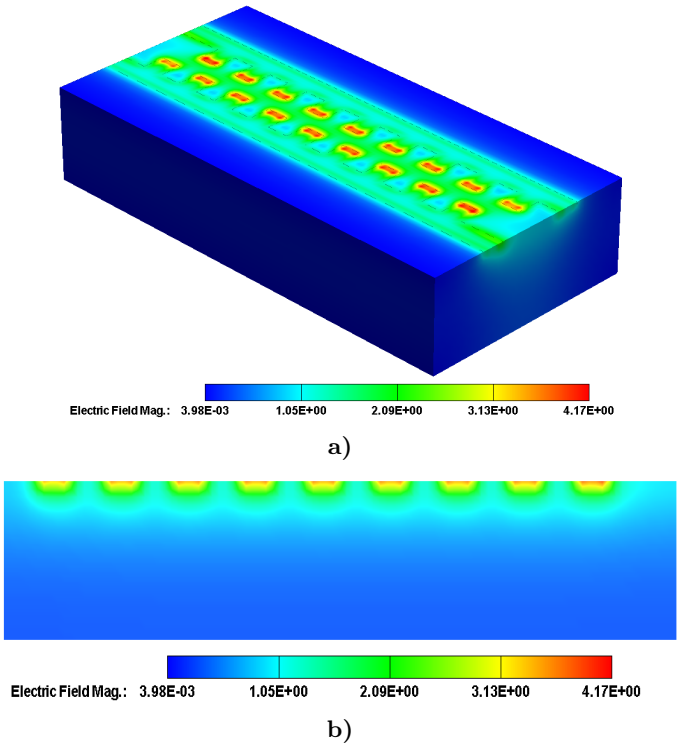

Fig. 10. Electric field distribution for 20 V applied voltage between castellated electrodes.

Coupled electrothermal simulation was performed to characterize the Joule heating. In Figure 11 variation of temperature as function of applied voltage is presented. For 10 V no significant heat is generated, while for 50 V the temperature can reach 50°C.

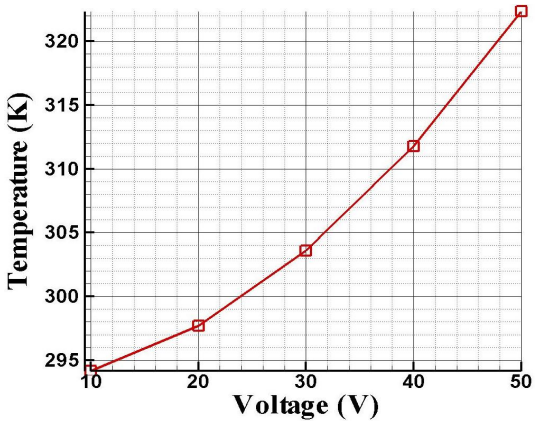

Fig. 11. Temperature variation (K) as function of applied voltage.

Figure 12 shows the thermal distribution corresponding to 50 V. In case of no flow (Figure 12a) the temperature can be considered uniform, since the change is bellow 0.1 K. In case with flow at $\Delta P = 10$ Pa between inlet and outlet (Figure 12b), the distribution is quasiuniform except the inlet region where the fluid has room temperature.

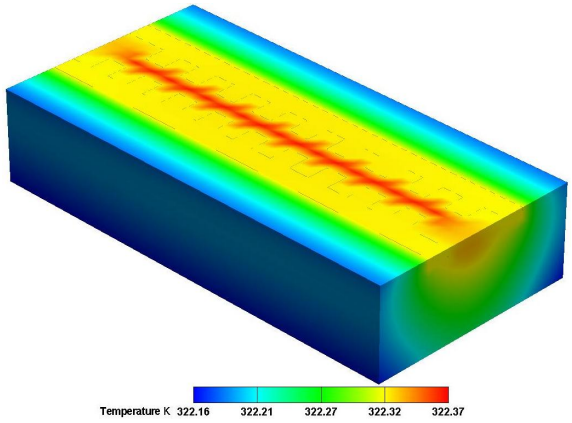

a)

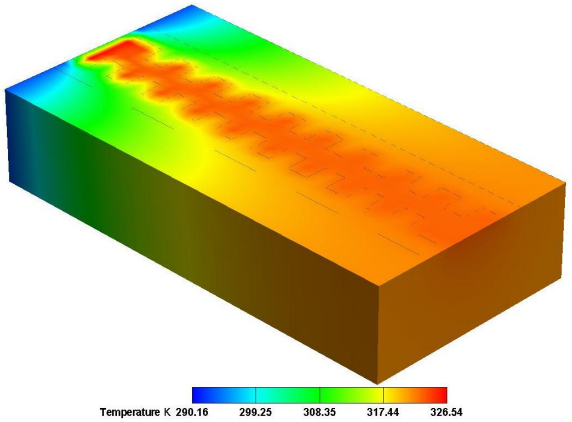

b)

Fig. 12. Temperature distribution [K] at 50 V applied (a) no flow (b) with flow ($\Delta P = 10$ Pa).

The numerical results for electric field were used to obtain the reaction force and particles DEP velocity and mobility. The solution flow was simulated using Comsol Mixture Model. The reaction force was introduced as body force and the DEP velocity as relative velocity between particles and fluid. As boundary conditions, a pressure drop of 10 Pa were applied between inlet and outlet and 0.31 volume fraction of particles at inlet, equivalent to 1 nMole concentration of particles with 1 μm diameter and 1 μMole concentration of particles with 0.1 μm diameter.

Figure 13 illustrates the distribution of concentration for 10 V and 50 V applied between electrodes, In case of 10 V applied, particles are separated in a larger area along the top surface, while for 50 V applied the separation area is smaller. This is due to higher DEP velocity and force as consequence of higher electric field and also to changes in material properties induced by heating, particularly to conductivity increasing. The fluid density and viscosity that are reduced by heating lead to a higher convection velocity which contribute to total velocity of particles; the comparison between the figures show also that the DEP velocity increase more than convection velocity, and at higher voltage, the contribution of convection velocity to total particles velocity becomes smaller than the contribution at low voltage.

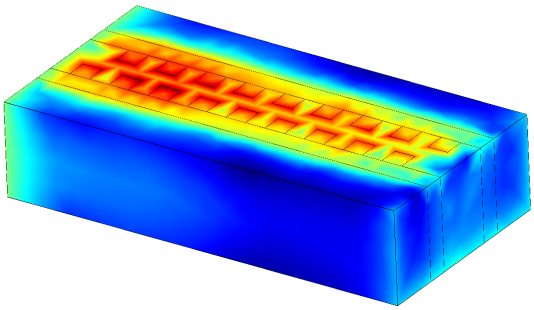

a)

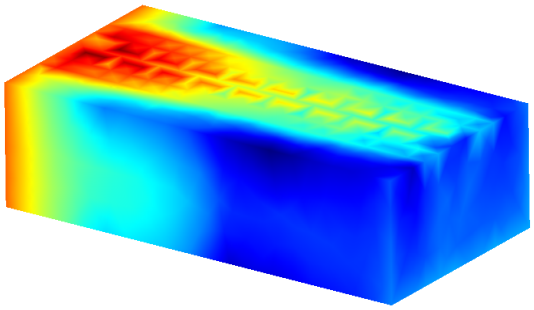

b)

Fig. 13. Concentration distribution of particles (1 μm diameter) at $\Delta P = 10$ Pa and positive DEP at 100 Hz; (a) 10 V; (b) 50 V.

The relative contribution of DEP and convective velocity is slightly changed for particles with 0.1 μm diameter, as illustrated in Figure 14. In this case, the convective velocity has a greater influence at high voltage than in case of particles with 1 μm diameter, due to the fact that for smaller particles, the DEP velocity depending on particle volume decreases with three orders of magnitude. Also, the differences between diffusion coefficients given by distinct particles sizes become greater at higher voltage due to temperature changes, and particles with smaller size will diffuse faster in the channel.

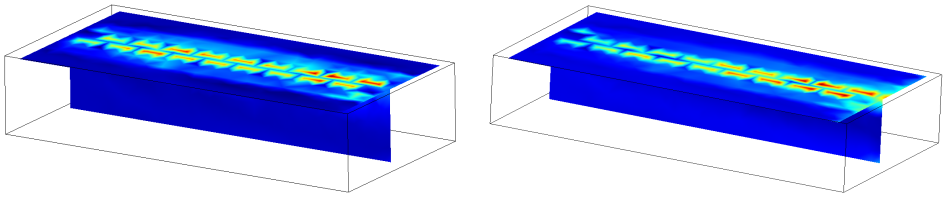

a) **b)**

Fig. 14. Concentration distribution of particles (0.1 μm diameter) at $\Delta P = 10$ Pa and positive DEP at 100 Hz; (a) 10 V; (b) 50 V.

In Figure 15 the influence of particles dielectrophoretic migration on fluid flow, modelled as reaction force is illustrated by streamlines that denotes the points with constant velocity. For comparison, Figure 15a shows the streamlines in case of no reaction force is taken into account; these are parallel to channels walls and each of them denotes a specific value of velocity from maximum in the middle to minimum near channel walls, according to parabolic flow profile.

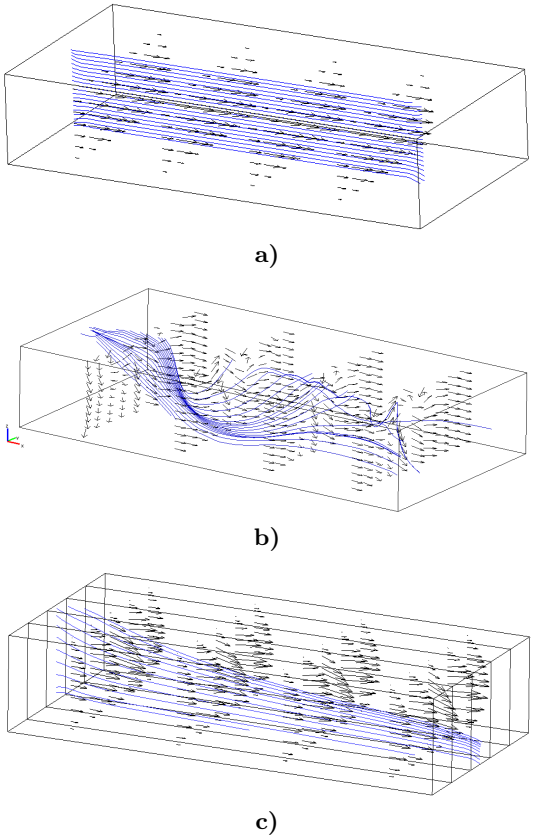

a)

b)

c)

Fig. 15. Velocity profile: streamlines and vectors orientation a) no reaction force; b) with reaction force, 10 V applied; b) with reaction force, 50 V applied.

Figures 15b and 15c, depict streamlines and velocity vector that correspond to 10 V and 50 V applied, and show the influence of particle DEP migration on fluid velocity. The profile is no longer parabolic, since the flow direction is modified by reaction force. The particles migrate towards the regions with higher values of electric field, and the reaction force modifies the profile and the fluid changes its flow direction in the opposite sense of particle migration. The difference between the actual modified profile and classic parabolic profile is higher in the region where particles concentration and dielectrophoretic force are higher, while in regions with lower concentration, the flow profile becomes similar to classic case.

4. Conclusions

Joule-heating induced effects on particles DEP separation are described as function of applied voltage. These effects were studied for a specific microfilter with planar castellated electrodes placed on a separation channel and were simulated using commercial software packages. A reaction force that describes the fluid response to particle dielectrophoretic migration was used in flow equations. The numerical results show that thermal variations induce changes in dielectrophoretic force and velocity, in flow characteristics and in particles diffusion, that lead to various ways of particles distribution and separation in the specific regions that depend also on particle size. By considering these additional phenomena as electrothermal effect and particle-fluid interaction we obtained distinct results by comparison to simplified approach. These results could explain some experimental observations that has not been expected and are not explained for simple dielectrophoresis, such as curly flow patterns in the regions of higher electrical field, that were observed for field strengths over 10^6 Vm^{-1} [8], values that are similar to those in our study. It was also observed that the magnitude of the effect vary with applied potential, and the direction of the rolls changes as function of frequency of the applied field. The flow pattern obtained by using presented models in our simulations demonstrate that particle migration influences the flow profile and the streamlines are modified by comparison to classic flow. The results can be used to predict the particles distribution with higher accuracy and therefore to optimize at virtual level, the design parameters of microfilters based on dielectrophoresis in order to improve the separation efficiency. Particularly, thermal effect on diffusion coefficient variation can be exploited to separate similar dielectric particles with different size based on increased difference between their diffusivity.

Acknowledgements. The research presented in this paper is supported by the Sectorial Operational Programme Human Resources Development (SOP HRD), financed from the European Social Fund and by the Romanian Government under the contract number POSDRU /89/1.5/S/63700.

References

[1] Furuta Y., Nishikawa H., Satoh T., Ishii Y., Kamiya T., Nakao R., Uchida S., *Fabrication and evaluation of 3D-electric micro filters using proton beam writing*,

Microelectronic Engineering, **86** (2009), pp. 1396–1400.

[2] Wakizaka Y., Hakoda M., Shiragami N., *Effect of electrode geometry on dielectrophoretic separation of cells*, Biochemical Engineering Journal, **20** (2004), pp. 13–19.

[3] Li H., Bashir R., *On the Design and Optimization of Micro-Fluidic Dielectrophoretic Devices: A Dynamic Simulation Study*, Biomedical Microdevices, **6**:4 (2004), pp. 289–295.

[4] Pham P., Texier I., Perraut F., *From Numerical to Experimental Study of Microsystems for Dielectrophoresis on Bioparticles*, Proceedings of the COMSOL Users Conference Paris, 2006.

[5] Ai Y., Beskok A., Gauthier D. T., Joo S. W., Qian S., *DC electrokinetic transport of cylindrical cells in straight microchannels*, Biomicrofluidics, **3** (2009), p. 044110-1-16.

[6] Castellanos A., Ramos A., Gonzalez A., Green N. G., Morgan H., *Electrohydrodynamics and dielectrophoresis in microsystems: scaling laws*, J. Phys. D: Appl. Phys., **36** (2003), pp. 2584–2597.

[7] Kang Y., Li D., *Electrokinetic motion of particles and cells in microchannels*, Microfluid Nanofluid, **6** (2009), pp. 431–460.

[8] Green N. G., Ramos A., Morgan H., *Ac electrokinetics: a survey of sub-micrometre particle dynamics*, J. Phys. D: Appl. Phys., **33** (2000), pp. 632–641.

[9] Hughes M. P., *Nanoelectromechanics in Engineering and Biology*, CRC Press, Boca Raton, 2003.

[10] Li D. (Editor), *Encyclopedia of Microfluidics and Nanofluidics*, Vol. **2**, Springer, 2008.

[11] Nedelcu O. T., *Study of particle-fluid interaction and thermal effects in dielectrophoretic microfilters*, Proc. of International Semiconductor Conference, 17–19 October 2011, Sinaia, Romania, pp. 113–116.

[12] Nedelcu O. T., *Design and Coupled Electro-Fluidic Simulation of a Novel Dielectrophoretic Microfilter*, Acta Physica Polonica A, Vol. **120** (2011), No. 6, pp. 1018–1020.

[13] Nguyen N.-T., Werely S. T. (Editors), *Fundamentals and applications of microfluidics*, Second Edition, Artech House Boston / London 2006.

[14] Coventorware documentation, *Analyzer Reference*, Version 2010.

[15] Comsol Multiphysics documentation, *Chemical Engineering Module – Users Guide*, Version 3.5, 2008.